Biosensors and Bioelectronics 121 (2018) 41–46

Contents lists available at ScienceDirect

Biosensors and Bioelectronics

journal homepage: www.elsevier.com/locate/bios

Graphene nanocomposites modified electrochemical aptamer sensor for rapid and highly sensitive detection of prostate specific antigen

Bo Wei[a], Kang Mao[b], Na Liu[a], Man Zhang[a,*], Zhugen Yang[c,*]

[a] Department of Thoracic Surgery, Beijing Shijitan Hospital, Capital Medical University, Beijing 100038, People's Republic of China
[b] College of Urban and Environmental Sciences, Peking University, Beijing 100871, People's Republic of China
[c] School of Engineering, University of Glasgow, Oakfield Avenue, Glasgow G12 8LT, United Kingdom

ARTICLE INFO

Keywords:
Electrochemical aptamer sensors
Paper microfluidic device
Graphene nano-composites
Screen-printing
Cancer diagnosis

ABSTRACT

Prostate specific antigen (PSA) is a widely used marker for the diagnosis of prostate cancer, and the increasing attention has been attracted on the development of rapid assay using biosensing technology. However, it remains challenging for the sensitive and selective detection of PSA in clinical samples. Here, we report a label-free microfluidic paper-based analytical device for highly sensitive electrochemical detection of PSA. The paper device was fabricated with wax printing to generate hydrophobic and hydrophilic layers for the construction of microfluidic channel, followed by screen-printing of three electrodes including working, counter and reference electrode. Gold nanoparticles (AuNPs)/reduced graphene oxide (rGO)/thionine (THI) nano composites were synthesized and characterized, which were coated onto working electrodes for the immobilization of DNA aptamer probe. THI servers as the electrochemical mediator to transduce the biological recognition between DNA aptamer and PSA, and the excellent conductivity of AuNPs and rGO also play a significant role of electron transfer, leading to a sensitive detection for PSA, able to detect PSA as low as 10 pg mL^{-1}, with a linear range from 0.05 to 200 ng mL^{-1}. We demonstrated that our electrochemical sensor for the detection of clinical serum samples, indicating that our sensor would provide a new platform for low cost, sensitive and point-of-care diagnosis of prostate cancer.

1. Introduction

Cancer is the major cause for the deaths worldwide (Siegel et al., 2017), and prostate cancer that targets the prostate gland, is a third leading cause of cancer mortality in men (Nelson et al., 2003). However, currently there are still no effective cures for the advanced metastatic stage of prostate cancer (Vassilikos et al., 2000; Huang et al., 2006; Geifman and Butte, 2016). Early and accurate diagnosis can increase the chances of successful treatment, which also provide the possibility to prolong the survival time (Mahal et al., 2016). Prostate specific antigen (PSA) is considered as the best serum biomarker available for the early detection of prostate cancer (Chen et al., 2012; Stock et al., 2015). The PSA level increases with advancing clinical stage and is proportional to the estimated volume of the tumor (Xie et al., 2016). In general, the level of PSA from 4 ng mL^{-1} in a human serum sample is usually regarded as the cut-off value for potential diagnosis as prostate cancer (Yang et al., 2015). To this end, the ultrasensitive, highly selective and point-of-care detection of PSA is essential for early cancer diagnosis (Grubisha et al., 2003; Spain et al., 2016).

Currently, the detection of PSA in the serum occurs at dedicated centralized laboratories using a large automated analyzer (Khan et al., 2018), requiring additional sample transportation, which is usually time-consuming and costly (Mueller-Lisse et al., 2002). In the past few years, a lot of methods such as enzyme-linked immunosorbent assay (ELISA) (Murphy et al., 2010), time-resolved fluorescence assay (Härmä et al., 2015), chemiluminescence immunoassay (Zhang et al., 2008; Liu, Fang et al., 2016), bioluminescent immunoassay (Ito et al., 2007) and electrochemical immunoassay (Jolly et al., 2016) have been developed for the detection of PSA based on the immunoreaction in a tedious and expensive way. On the contrary, the development of a biosensors for PSA detection will offers a great possibility for creating a low-cost and highly sensitive point-of-care testing (POCT) of PSA in real time (Healy et al., 2007). This would also drastically decrease the need for sample transportation to the central laboratories, which is very helpful to build a new economic way for healthcare system (Lilja et al., 2008). Compared to other methods, the electrochemical sensors have shown great advantages, such as fast response time, low cost, and less or minimal sample processing (Li et al., 2014).

* Corresponding authors.
E-mail addresses: mzhang99@aliyun.com (M. Zhang), zhugen.yang@glasgow.ac.uk (Z. Yang).

https://doi.org/10.1016/j.bios.2018.08.067
Received 2 July 2018; Received in revised form 16 August 2018; Accepted 27 August 2018
Available online 30 August 2018

Most of the detection methods for PSA are based on antibodies due to their high selectivity toward the antigen (Chen et al., 2014). However, antibodies are larger molecules and have greater peptidase susceptibility and immunogenicity, which may limit its applications (Murphy et al., 2015). Compared with antibodies, nucleic-acid aptamers, which are selected by a technology called SELEX (Systematic Evolution of Ligands by Exponential Enrichment) in vitro, have recently attracted more and more attention, due to low cost, stability and being easy to synthesize (Keefe and Cload, 2008; Sefah et al., 2010). Their well-defined structures enable their efficient recognition with the targets, including small molecules, peptides and proteins, with an excellent affinity and specificity. More importantly, they would offer remarkable flexibility and convenience in the design of their structures, which has led to higher sensitivity and selectivity for the development of novel biosensors (Savory et al., 2011). It is easy to modify aptamers chemically with plenty of functional groups, such as biotin, amine and thiol groups on its 5′ end, enabling for the immobilization of probes for the biosensors chip (Ohno et al., 2010).

Paper is a biocompatible porous cellulose fiber web with large surface area, and the porous nature fulfills the primary tasks such as diagnostic tests using body fluids and fluid transport (Liana et al., 2012; Nery et al., 2013). Since microfluidic paper-based analytical devices (μPADs) were first reported by Whitesides' group, they were increasingly recognized as ideal platforms designed for POCT (Martinez et al., 2010). μPADs have demonstrated excellent properties, including low sample and reagent consumption, low cost, small size, portable and easy-to-operate. What's more, μPADs can be fabricated in bulk using less expensive means, including photolithography, inkjet etching and printing (Li et al., 2013). Among various methods, wax-printing is considered as the cheapest and most easily implemented means of mass production available, and has recently been shown to be very effective in the production of PADs at minute cost (X. Wang et al., 2016; Y. Wang et al., 2016).

Nanotechnology is playing a significant role in fabrication of sensitive biosensors. Currently, more and more nanomaterials have been developed to improve the sensitivity and specificity of target detection (Wang et al., 2018). Compared with traditional sensors, nanomaterials modified electrochemical biosensors not only possessed large surface area and favorable microenvironment, but also exhibited remarkable conductivity, stability and excellent biocompatibility (Yang et al., 2017). For example, graphene, a two-dimensional nano carbon material with extraordinary physical and chemical properties, has been one of the most promising materials in designing electrochemical biosensors (X. Wang et al., 2016; Y. Wang et al., 2016). Besides, gold nanoparticles (AuNPs), one of the metallic nanoparticles, possess large specific surface area, good biocompatibility and high surface free energy. They are able to be bond with functional groups such as amino group (–NH_2) and mercapto group (–SH) (Ding et al., 2017). Moreover, the nanohybrids of graphene with gold nanostructure has combined all the advanced properties and/or even enhanced the performance for the sensing due to the synergetic interaction. For example, the nanohybrids can not only efficiently immobilize the biological receptor but also limit the non-specific adsorption, which will significantly improve the sensitivity of biosensors (Singh and Singh, 2013).

In this paper, we proposed a low cost, label-free, highly sensitive and selective electrochemical aptamer sensor to detect PSA in serum samples using disposable paper microfluidic device. We fabricate the paper-based sensor with wax-printing and screen-printing. The AuNPs/rGO/THI were synthesized and well characterized for the surface modification of paper electrodes. DNA aptamer was immobilized onto the nanomaterial coated paper electrodes for the specifically recognition of PSA. We optimized the condition to sensitively detect PSA as low as 10 pg mL^{-1}, also enabling the detection of the clinical serum samples. Experimental results demonstrated that our electrochemical sensors had a great potential for the detection of clinical sample in a rapid and low-cost way and our sensors could be used as POCT for cancer diagnosis.

2. Experimental section

2.1. Apparatus

The Gamry electrochemical potentiostat was used to carry out electrochemical measurements, including differential pulse voltammetry (DPV) and cyclic voltammetry (CV) (Gamry Reference 600, Gamry Instruments, Warminster, PA, USA). A three-electrode system was integrated into the microfluidic paper-based device. Deionized water was purified through a Michem ultrapure water apparatus (Michem, Chengdu, China, resistivity > 18 MΩ cm^{-1}). The morphology of composites was characterized by A JEOL-100CX transmission electron microscope (TEM) (H7650, Hitachi, Japan). A Xerox ColorQube 8570 digital wax printer was used to spray wax on the surface of paper. Other apparatus in this study included oven from Yiheng (DHG-9023A, Yiheng, Shanghai, China) and ultrasonic generator from Hechuang (China).

2.2. Reagents

DNA aptamer against PSA: 5′-ATT AAA GCT CGC CAT CAA ATA GC-3′ (Mw 7196.85 g mol^{-1}) were synthesized and purified by Sangon Biotechnology Co. Ltd. (Shanghai, China). In addition, anti-PSA apatmer was modified with a thiol group to be immobilized onto electrodes for DPV measurement. PSA and Tris-Ethylenediaminetetraacetic acid (EDTA) buffer solution (10 mMTris-HCl + 1 mM EDTA, pH = 8.0) were purchased from Shanghai Sangon Biotechnology Co. Ltd. Thionine acetate was purchased from Alfa Aesar. 6-mercaptohexanol (MCH) was provided by Sigma-Aldrich (USA). Reduced graphene oxide (rGO) was bought from Xianfeng Nanomaterials Company (Nanjing, China). Whatman chromatography paper NO. 1 (pure cellulose paper) was obtained from GE Healthcare Worldwide and used with further adjustment of size. The conductive carbon ink (ED581ss) was received from Acheson and Ag|AgCl ink (CNC-01) was from Yingman Nanotechnology Company. All other chemicals were of reagent grade and used as received. All solutions were prepared using deionized water. Clinical serum samples were provided by Beijing Shijitan Hospital, Capital Medical University (Beijing, China).

2.3. Fabrication of the paper-based electrodes

A simple illustration of the microfluidic paper-based analytical device was shown in Scheme 1. The device, which consisted of two layers, was fabricated on two pieces of cellulose filter papers. The specific size of the device was 10.5 mm × 30.0 mm. By adopting this size, the device could be easily inserted into a backend interface and then a portable electrochemical reader, enabling a rapid test even at low setting areas. The workflow of the paper-based sensor was described as following, the samples were introduced from the inlet, and then the filtered samples flowed through the microchannel and were recognized by the DNA aptamer on the electrodes. As paper is made of fibers and rich of porous structures, the samples can permeate through the paper, reaching the surface of the working electrode for the electrochemical detection.

The structures, including microfluidic channels and electrodes were designed by the Adobe Illustrator CS5 software. During design, some factors were taken into consideration, such as detection convenience and so on. The designed patterns were shown in Scheme 1. As we can see, the counter electrode and the reference electrode were in one layer. They were grouped together, forming a circle in the middle, whose diameter was 2 mm. The working electrode was in another layer, whose diameter is also 2 mm. Besides, registration marks were designed on each layer to ensure assembly accuracy.

After structural design, a Xexro digital wax printer was used to

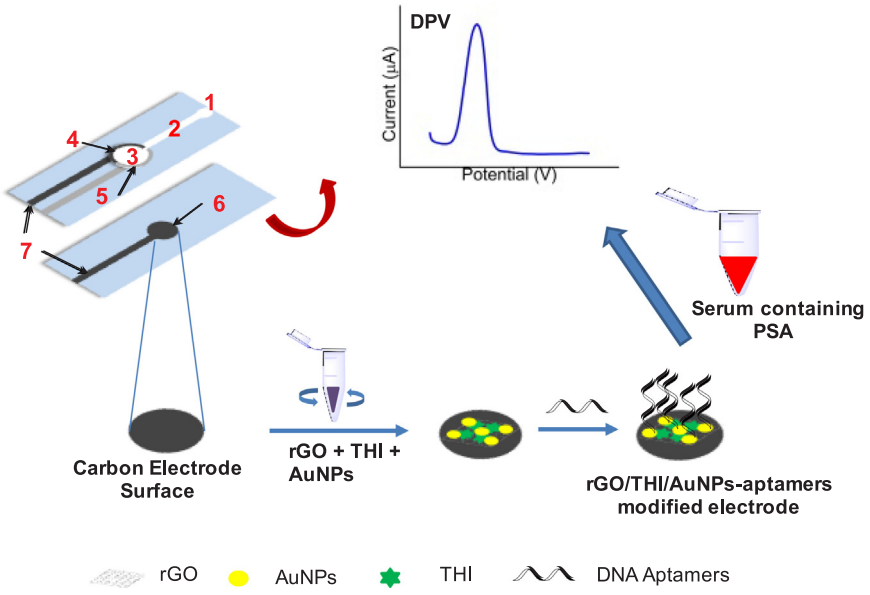

Scheme 1. Fabrication and modification process of the microfluidic paper-based aptasensor and the typical response of the detection of analyte (1) injection port; (2) microfluidic channel; (3) reaction site; (4) screen-printed carbon counter electrode; (5) screen-printed reference electrodes; (6) working electrode; (7) screen-printed electrode-lead.

pattern the microfluidic channels onto the surface of cellulose fiber papers (Scheme 1), and was heated at 140 °C for 1 min, and the wax would re-melt and penetrate into the porous filter paper to form the hydrophobic areas with a double-sided pattern. However, the unpattern white areas would still remain excellent hydrophilicity, thus forming the microfluidic channels. Afterwards, we printed three electrodes onto the surface of the above paper sheets by screen-printing technique. The working electrode and the counter electrode were of conductive carbon ink, while the reference electrode was of conductive Ag|AgCl ink, which will be ready for the coating to perform electrochemical detection. The device could offer a number of advantages, such as a certain amount of sample consumption, a small volume of required sample and a simple procedure of sample handling.

2.4. Synthesis and characterization of AuNPs/rGO/THI nanocomposites

The synthesis of AuNPs/rGO/THI nanocomposite was formed due to the π-π stacking interactions between benzene rings and the THI molecules, which contain benzene ring in their molecular structure and is able to non-covalently attach to the rGO. Positively charged thionine molecules enable negatively charged gold nanoparticles to bind with the anionic rGO surfaces.

The rGO/THI nanocomposite was carried out in a 100 mL round-bottom flask equipped with a magnetic stirrer. Briefly, the protocol for synthesizing the AuNPs/rGO/THI nanocomposite was described below: a total of 10 mg of rGO was mixed with 10 mL deionized water firstly and treated with ultrasonic wave for 1 h to obtain rGO suspension. And then 10 mL of 2 mg mL^{-1} THI solution was added to the above solution, followed by string under high agitation speed at room temperature overnight. The composites were centrifuged at 8000 rpm for 15 min and washed with deionized water to remove the non-integrated THI molecules. The obtained rGO/THI nanocomposites were redispersed in 2 mL deionized water. Under vigorously stirring, 10 mL of AuNPs solutions were injected slowly. The resulting suspension was stirred for 12 h at room temperature. The final mixture was centrifuged and purified, followed by washing with ethanol and water for times. The synthesized AuNPs/rGO/THI nanocomposites would be stored at 4 °C for further use.

2.5. Elaboration of the electrochemical aptamer sensors

The fabrication procedure of the microfluidic paper-based aptasensor was shown in Scheme 1. Firstly, 10 μL AuNPs/rGO/THI suspensions were transferred on the surface of the paper electrodes and then dried in an oven at 50 °C for half an hour. Subsequently, 10 μL of DNA aptamers solution was introduced onto the surface of AuNPs/rGO/THI modified SPCE and incubated overnight at 4 °C. As the aptamers had been modified with a thiol group, which is able to conjugate with AuNPs on the electrode surface. The concentration of the aptamer was optimized at 36 μg mL^{-1} to detect different concentrations of PSA. To block any possible remaining active sites and reduce non-specific adsorption, 10 μL of MCH solutions (1 mM) were added on the modified electrode surface and incubated at room temperature for 1 h. After that, the TE buffer (10 mM Tris-HCl, 1 mM EDTA, pH 7.4) was utilized to rinse the surface of the electrode, followed with storing at 4 °C for further use. To access the function of the developed electrochemical aptasensor, prior to electrochemical measurements, 10 μL of PSA solutions at a designed concentration were added onto the electrode surface to incubate for 1 h at room temperature.

2.6. Electrochemical measurements

All measurements used a three-electrode cell, with the nanocomposites modified SPCE as working electrode, the screen printed carbon electrode as counter electrode and the screen printed Ag/AgCl electrode as reference electrode, against which all potentials are quoted. Three electrodes were integrated together into a single paper-based aptasensor. Cyclic voltammetry (CV) and differential pulse voltammetry (DPV) measurements were performed using a Gamry electrochemical workstation in 0.1 M PBS solutions (pH = 7.4). DPV scans run between − 0.5 V and 0.3 V with settings of scan rate 0.05 V s^{-1}, step potential 0.005 V, modulation amplitude 0.05 V, modulation time 0.05 s and interval time 0.1 s. CV scans were conducted between − 0.5 V and 0.1 V, whose scan rate was 100 mV s^{-1}.

3. Results and discussion

3.1. Characterization of the paper electrodes surface

Fig. 1A illustrates TEM image of the synthesized rGO/THI nanocomposites and Fig. 1B shows the image of AuNPs/rGO/THI nanocomposites. Compared with rGO/THI nanocomposites, Fig. 1B confirms that gold nanoparticles are typically hybridized with rGO surface with dispersion. Free nanoparticles are nearly not present in the background of TEM images, indicating their strong interactions with rGO. The THI molecule, as an electrically active substance, is able to generate an

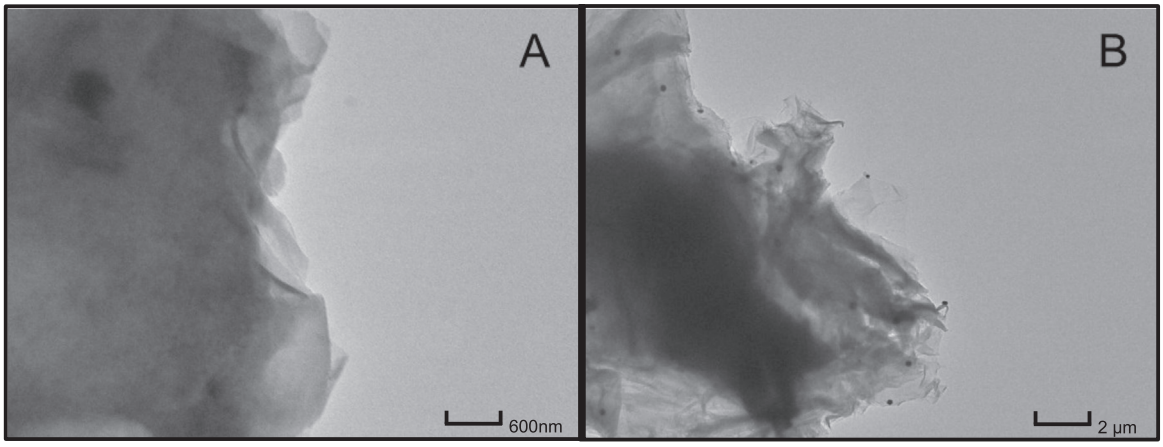

Fig. 1. TEM images of (A) rGO/THI and (B) AuNPs/rGO/THI nanocomposites.

electric current through redox reactions on the surface of the electrode. rGO, with favorable conductivity and biocompatibility, are usually adopted to fabricate electrochemical biosensors for improving electrochemical signals. Moreover, they will also introduce nano-porous structures to the surface of the electrode, which can remarkably increase not only the surface area, but also the specific surface area, resulting in a higher density load of electro-actively materials and a higher electrochemical response. The catalytic activity of gold is known to depend strongly on its size. Extremely small metal particles are of tremendous interest due to their unusual catalytic and optical properties. In this work, AuNPs with an average diameter of 15 nm were used for the hybridized, and it was anticipated not only to provide catalytic activity when attached to rGO, but also help to chemically bond with thiol groups modified aptamers.

3.2. Electrochemical responses of the paper-based aptasensor

In order to determine the basic electrochemical performance of the designed paper-based analytical device, typical electrochemical measurements including CV and DPV were performed. As shown in Fig. 2A, CV responses of the bared working electrode, AuNPs/rGO/THI and AuNPs/rGO/THI-aptamer modified electrodes were monitored in 0.1 M PBS (pH = 7.4) at a scan rate of 100 mV s^{-1}. Compared with bared electrode (black line), AuNPs/rGO/THI modified electrode (red line) provide a pair of pronounced redox peaks, which was attributed to the redox reactions of THI molecules on the surface of the electrode. The position of peak currents of reduction and oxidation were nearly the same though the electrodes were coated with different layers. The separation of the corresponding potentials ΔEp were at about 59 mV, indicating a promising reversible electrochemical redox-reduction process. The current response decreased after the introduction of DNA aptamers onto the electrode (pink curve), demonstrating the immobilization of aptamers through Au-S bond onto the electrodes surface. This is likely that the binding of aptamers onto the electrodes surface produced a steric hindrance, leading to a partial inhibition of electron transfer. After the electrochemical aptasensor was incubated with different concentrations of PSA, the peak currents further decreased. This may be associated with that the conjunction of DNA aptamer and PSA resulted in the enhanced steric hindrance, which was directly proportional to the concentrations of PSA, enabling to the quantification of PSA with our electrochemical sensors. With an increasing concentration of PSA, generating more aptamer-PSA complex, the peak current decreased.

DPV responses of the electrodes were shown in Fig. 2B. Due to the efficient redox-activity of THI and the excellent conductivity of rGO and AuNPs, a peak current at 15.97 μA was present for the AuNPs/rGO/THI nanocomposites modified aptasensor. Subsequently, the loading of aptamers led to a decrease of the redox peak current owing to the formation of a blocking layer for electron transfer. After incubated with a solution of 100 pg mL^{-1} PSA, the insulating protein layers on the electrode further prevent the electron transfer. The peak currents decreased to 9.76 μA. This indicates that the difference of the current peak value is

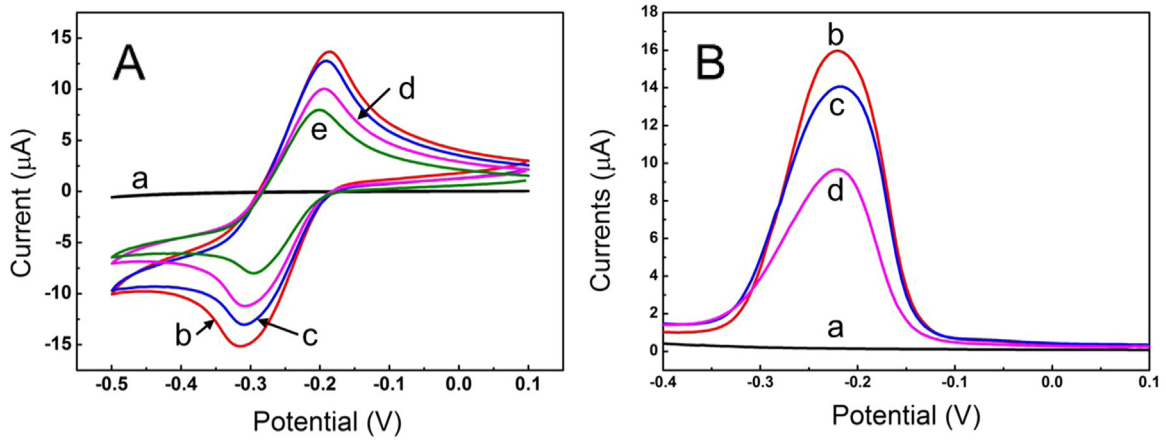

Fig. 2. Basic responses of the aptasensor monitored in 0.1 M PBS solution, pH = 7.4. (A) CV responses of the paper-based aptasensor: a) bare working electrode; b) AuNPs/rGO/THI nanocomposites modified electrode; c) AuNPs/rGO/THI-aptamer modified electrode; d) the aptasensor incubated with 100 pg mL^{-1} PSA; e) the aptasensor incubated with 1 ng mL^{-1} PSA; (B) DPV responses of the aptasensor: a) bare working electrode; b) AuNPs/rGO/THI nanocomposites modified electrode; c) AuNPs/rGO/THI-aptamer modified electrode; d) the aptasensor incubated with 100 pg mL^{-1} of PSA.

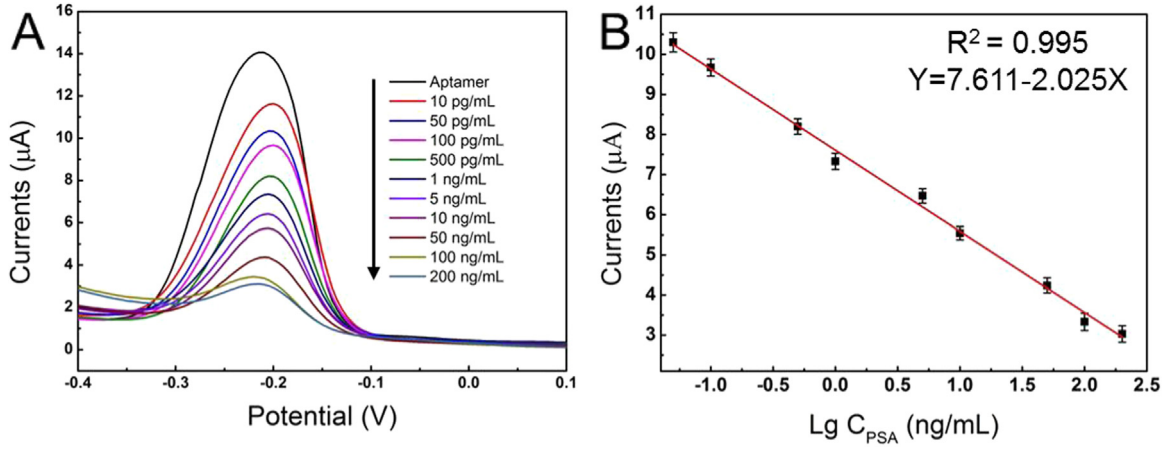

Fig. 3. (A) DPV responses to different concentrations of PSA in 0.1 M PBS solution, pH = 7.4; (B) The calibration curve of the paper-based electrochemical aptasensor between the current peak and the various concentrations PSA.

proportional to the concentration of PSA, enabling our proposed electrochemical sensors to detect PSA. Additionally, the repeatability of the aptasensor was also evaluated as it is a crucial parameter for disposable paper sensors. As shown in Fig. S1, different sensors show similar electrochemical response and the relative standard deviation from four-time measurement was 1.06%, indicating our sensors have a promising repeatability.

3.3. Detection of PSA with the paper-based electrochemical aptasensor

Under optimal experiments conditions, the analytical performance such as sensitivity and dynamic range of the aptasensor for PSA detection are evaluated in 0.1 M PBS solutions. The electrochemical aptasensor was incubated with various concentrations of PSA, and scanned by DPV. Each measurement was performed before the conjugation with PSA as the initial response. As shown in Fig. 3A, the currents decreased gradually with the increasing PSA concentrations. Based on the signal-to-noise ratio method using a factor of 3, the limit of detection (LOD) was estimated to be 10 pg mL^{-1}, and the dynamic range was determined as from 0.05 ng mL^{-1} to 200 ng mL^{-1} (R^2 = 0.995). The regression equation obtained between the currents and the concentration of analytes was I_{dpv} (μA) = 7.6–2.0 lg C_{PSA} (ng mL^{-1}). Typically, a PSA level of 4 ng mL^{-1} in a human serum sample is usually regarded as the cut-off value for potential diagnosis of prostate cancer, and our proposed paper sensor has an even lower LOD thus will provide a promising tool for the detection of PSA in clinical sample for diagnosis.

In order to access the binding specificity of the aptasensor towards PSA, some potential interference, including carcinoembryonic antigen (CEA), neuron-specific enolase (NSE), ascorbic acid (AA), bovine serum albumin (BSA) and immunoglobulin G (IgG) were tested for the evaluation of the selectivity. As shown in Fig. 4A, a significant decrease of currents induced by the aptasensor with 1 ng mL^{-1} PSA, while the responses of the interfering proteins were nearly the same as the blank. It was suggested that our electrochemical aptasensor had good specificity towards PSA. In addition, another study was carried out in a mixture condition to further explore the selectivity. 1 ng mL^{-1} of AA, IgG, NSE, CEA and BSA were added separately into 1 ng mL^{-1} PSA solution. Even though these interferences coexisted in the detection of PSA, the variations of peak currents were 7.24%, 6.81%, 5.52%, 3.59% and 6.22%, respectively, showing negligible changes. These data demonstrated that our proposed paper-based aptasensor are very selective for PSA detection.

Table S1 summarized the analytical performance of the developed sensors for the detection of PSA. Our electrochemical sensors show a promising sensitivity and dynamic range. More importantly, our electrodes were fabricated from paper, which is not only low cost, disposable and easy-to-use, but also sensitive and selective for the detection of protein cancer biomarkers such as PSA. Using conductive nanomaterial for the surface modification of electrodes and a selective and inexpensive DNA aptamer as the probe, we developed a label free electrochemical sensor for the sensitive detection of PSA, enabling rapid diagnosis of cancer and a wide biomedical application.

3.4. Analytical results of clinical serum samples

To further explore the feasibility of our aptasensor for clinical applications, human serum samples obtained from Shijitan Hospital were analyzed. The results of clinical serum samples from our proposed sensors were compared with reference values obtained by the electrochemiluminescence method (Roche, USA), which was performed in the hospital as a standard way. Seven samples with known PSA concentration ranging from 2.1 ng mL^{-1} to 91.3 ng mL^{-1} were detected firstly to obtain the linear fitting curve between the peak currents and the concentrations of PSA (Fig. S2). As shown in Table 1, the clinical serum samples were tested directly without any dilution and the analytical results were generally comparable with the reference values tested in the hospital. The relative errors between this work and the reference method are less than 8.81%, indicating that our aptasensors hold a great promise for the detection of PSA in clinical samples.

4. Conclusion

In summary, we have demonstrated low cost and label-free electrochemical aptamer sensors using paper microfluidic device for the sensitive detection of PSA in clinical samples. We use the wax-printed and screen-printing technology to fabricate the paper electrodes, and modify the surface with electrochemical active nanomaterials for the immobilization of aptamer probes for the highly sensitive and selective detection of PSA. The excellent conductivity of AuNPs/rGO/THI modified electrodes enables an effective electron transfer at the interference of the aptamer receptor and electrodes, inducing a specific peak current associated with electrochemical mediator of THI. However, upon binding with the analytes the decreasing of the peak current is proportional to the concentration of the PSA, allowing for the quantification of target. Under the optimized condition, our electrochemical aptamer sensor is able to detect as low as 10 pg mL^{-1} of PSA, with a dynamic range from 0.05 to 200 ng mL^{-1}, allowing for the detection of PSA in clinical samples. The testing of clinical serum samples shows a reasonable variation with a standard reference from the hospital. However, our sensors have a fast response time and low cost, providing a potential tool for the POCT for cancer diagnosis. More importantly,

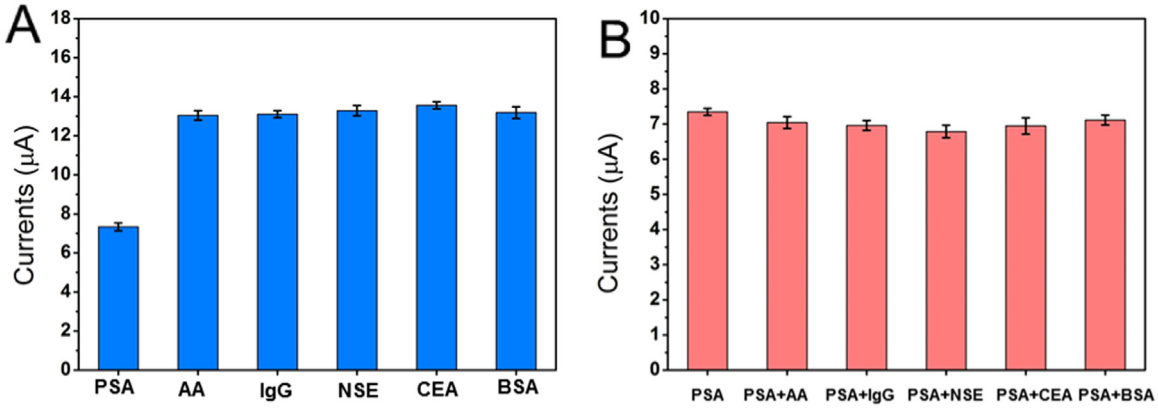

Fig. 4. The evaluation of the selectivity of the proposed aptasensors **(A)** DPV responses of the sensor to 1 ng mL^{-1} PSA and 1 ng mL^{-1}AA, IgG, NSE, CEA and BSA, respectively; (B) DPV responses of the aptasensor to 1 ng mL^{-1} PSA and 1 ng mL^{-1} PSA mixed with 1 ng mL^{-1}AA, IgG, NSE, CEA and BSA, respectively.

Table 1
Paper-based electrochemical aptamer sensors for the detection of PSA in clinical serum samples.

No.	Currents (μA)	Reference (ng mL^{-1})	This work (ng mL^{-1})	Relative errors (%)
1	6.72	1.12	1.03	− 8.04
2	6.65	3.06	2.91	− 4.90
3	6.57	4.72	4.85	2.75
4	6.54	5.15	5.48	6.41
5	6.49	7.17	6.65	− 7.25
6	6.45	8.08	7.73	− 4.33
7	6.40	9.06	8.89	− 1.88
8	6.32	10.50	11.05	5.24
9	6.34	11.13	10.58	− 4.94
10	6.24	12.12	12.97	7.01
11	6.27	12.79	12.18	− 4.77
12	6.19	13.12	14.28	8.84
13	6.16	14.57	15.08	3.50
14	6.15	15.45	15.13	− 2.07
15	6.10	17.31	16.47	− 4.85
16	5.93	20.42	20.76	1.67
17	5.78	25.13	24.34	− 3.14
18	5.12	38.92	40.69	4.55
19	4.34	61.43	60.22	− 1.97
20	4.12	70.24	65.55	− 6.68
21	3.75	78.72	74.85	− 4.92

our aptamer sensors can also be used as a generic platform for the detection of a range of analytes by adapting different aptamer probes, such as small molecules and proteins for biomedical and environmental application.

Acknowledgements

This work is sponsored Special funds for the Construction of High Level Health Technical Personal in Beijing, China, and Beijing Municipal Administrated Hospital Incubating Program, China (PX 2016044). ZY thanks the UK NERC Fellowship Grant (NE/R013349/1).

Appendix A. Supporting information

Supplementary data associated with this article can be found in the online version at doi:10.1016/j.bios.2018.08.067.

References

Chen, X., Zhou, G., Song, P., Wang, J., Gao, J., Lu, J., Fan, C., Zuo, X., 2014. Anal. Chem. 86 (15), 7337–7342.
Chen, Z., Lei, Y., Chen, X., Wang, Z., Liu, J., 2012. Biosens. Bioelectron. 36 (1), 35–40.
Ding, S., Mosher, C., Lee, X.Y., Das, S.R., Cargill, A.A., Tang, X., Chen, B., Mclamore, E.S., Gomes, C., Hostetter, J.M., 2017. Acs Sens 2 (2), 210.
Geifman, N., Butte, A.J., 2016. Sci. Data 3.
Grubisha, D.S., Lipert, R.J., Park, H.Y., Driskell, J., Porter, M.D., 2003. Anal. Chem. 75 (21), 5936.
Härmä, H., Soukka, T., Lönnberg, S., Paukkunen, J., Tarkkinen, P., Lövgren, T., 2015. Lumin. J. Biol. Chem. Lumin. 15 (6), 351–355.
Healy, D.A., Hayes, C.J., Leonard, P., Mckenna, L., O'Kennedy, R., 2007. Trends Biotechnol. 25 (3), 125–131.
Huang, L., Reekmans, G., Saerens, D., Friedt, J.M., Frederix, F., Francis, L., Muyldermans, S., Campitelli, A., Van, H.C., 2006. Biosens. Bioelectron. 21 (3), 483–490.
Ito, K., Nishimura, W., Maeda, M., Gomi, K., Inouye, S., Arakawa, H., 2007. Anal. Chim. Acta 588 (2), 245–251.
Jolly, P., Tamboli, V., Harniman, R.L., Estrela, P., Allender, C.J., Bowen, J.L., 2016. Biosens. Bioelectron. 75, 188.
Keefe, A.D., Cload, S.T., 2008. Curr. Opin. Chem. Biol. 12 (4), 448–456.
Khan, M.S., Dighe, K., Wang, Z., Srivastava, I., Daza, E., Schwartz-Dual, A.S., Ghannam, J., Misra, S.K., Pan, D., 2018. Analyst 143.
Li, L., Li, W., Ma, C., Yang, H., Ge, S., Yu, J., 2014. Sens. Actuators B Chem. 202 (4), 314–322.
Li, W., Li, L., Li, S., Wang, X., Li, M., Wang, S., Yu, J., 2013. Sens. Actuators B Chem. 188 (11), 417–424.
Liana, D.D., Raguse, B., Gooding, J.J., Chow, E., 2012. Sensors 12 (9), 11505.
Lilja, H., Ulmert, D., Vickers, A.J., 2008. Nat. Rev. Cancer 8 (4), 268–278.
Liu, A., Fang, Z., Zhao, Y., Li, S., Liu, S., 2016. Biosens. Bioelectron. 81, 97–102.
Mahal, B.A., Aizer, A.A., Efstathiou, J.A., Nguyen, P.L., 2016. Cancer 122 (1), 78–83.
Martinez, A.W., Phillips, S.T., Butte, M.J., Whitesides, G.M., 2010. Angew. Chem. 119 (8), 1340–1342.
Mueller-Lisse, U.G., Mueller-Lisse, U.L., Haller, S., Schneede, P., Scheidler, J.E., Schmeller, N., Hofstetter, A.G., Reiser, M.F., 2002. J. Comput. Assist. Tomogr. 26 (3), 432–437.
Murphy, G.P., Holmes, E.H., Boynton, A.L., Kenny, G.M., Ostenson, R.C., Erickson, S.J., Barren, R.J., 2010. Prostate 26 (3), 164–168.
Murphy, G.P., Tino, W.T., Holmes, E.H., Boynton, A.L., Erickson, S.J., Bowes, V.A., Barren, R.J., Tjoa, B.A., Misrock, S.L., Ragde, H., 2015. Prostate 28 (4), 266–271.
Nelson, W.G., De Marzo, A.M., Isaacs, W.B., 2003. N. Engl. J. Med. 349 (4), 366.
Nery, W. Emilia, Kubota, Lauro, T., 2013. Anal. Bioanal. Chem. 405 (24), 7573–7595.
Ohno, Y., Maehashi, K., Matsumoto, K., 2010. J. Am. Chem. Soc. 132 (51), 18012–18013.
Savory, N., Abe, K., Sode, K., Ikebukuro, K., 2011. Biosens. Bioelectron. 26 (4), 1386–1391.
Sefah, K., Shangguan, D., Xiong, X., O'Donoghue, M.B., Tan, W., 2010. Nat. Protoc. 5 (6), 1169.
Siegel, R.L., Miller, K.D., Jemal, A., 2017. Ca A Cancer J. Clin. 67 (1), 7.
Singh, V., Singh, D., 2013. Process Biochem. 48 (1), 96–102.
Spain, E., Gilgunn, S., Sharma, S., Adamson, K., Carthy, E., O'Kennedy, R., Forster, R.J., 2016. Biosens. Bioelectron. 77, 759–766.
Stock, R.G., Stone, N.N., Dewyngaert, J.K., Lavagnini, P., Unger, P.D., 2015. Cancer 77 (11), 2386–2392.
Vassilikos, E.J., Yu, H., Trachtenberg, J., Nam, R.K., Narod, S.A., Bromberg, I.L., Diamandis, E.P., 2000. Relapse and cure rates of prostate cancer patients after radical prostatectomy and 5 years of follow-up. Clin. Biochem. 33 (2), 115–123.
Wang, X., Deng, W., Shen, L., Yan, M., Yu, J., 2016a. New J. Chem. 40 (3), 2835–2842.
Wang, Y., Luo, J., Liu, J., Li, X., Kong, Z., Jin, H., Cai, X., 2018. Biosens. Bioelectron. 107, 47–53.
Wang, Y., Xu, H., Luo, J., Liu, J., Wang, L., Fan, Y., Yan, S., Yang, Y., Cai, X., 2016b. Biosens. Bioelectron. 83, 319–326.
Xie, Y., Wei, X., Yang, Q., Guan, Z., Liu, D., Liu, X., Zhou, L., Zhu, Z., Lin, Z., Yang, C., 2016. Chem. Commun. 52 (91), 13377.
Yang, T., Gao, Y., Liu, Z., Xu, J., Lu, L., Yu, Y., 2017. Sens. Actuators B Chem. 239, 76–84.
Yang, Z., Kasprzyk-Hordern, B., Goggins, S., Frost, C.G., Estrela, P., 2015. Analyst 140 (8), 2628–2633.
Zhang, X.F., Liu, Y.B., Jia, J.J., Wen-Ge, X.U., Zi-Ying, L.I., Chen, Y.L., Han, S.Q., 2008. At. Energy Sci. Technol.